Vibrational and Thermal Properties of Crystalline Topiramate

Diniz M. Sena Jr.,[a] Paulo T. C. Freire,*,[b] Josué M. Filho,[b] Francisco E. A. Melo,[b]
Fenelon M. Pontes,[c] Elson Longo,[d] Odair P. Ferreira[e] and Oswaldo L. Alves[e]

[a]*Universidade Regional do Cariri, 63105-000 Crato-CE, Brazil*

[b]*Departamento de Física, Universidade Federal do Ceará, 60455-760 Fortaleza-CE, Brazil*

[c]*Faculdade de Ciências, Universidade Estadual Paulista, Bauru-SP, Brazil*

[d]*Instituto de Química, Universidade Estadual Paulista, PO Box 355, 14801-970 Araraquara-SP, Brazil*

[e]*Laboratório de Química do Estado Sólido, Instituto de Química, Universidade Estadual de Campinas,*
CP 6154, 13081-970 Campinas-SP, Brazil

O topiramato, que é uma poderosa droga anticonvulsiva utilizada para controlar os sintomas da epilepsia, foi investigado pelas técnicas de difratometria de raios X, FT-Raman, FT-infravermelho, análise termogravimétrica, análise térmica diferencial e cálculos com teoria do funcional de densidade. A partir deste estudo foi possível identificar a maior parte das bandas observadas nos espectros Raman e infravermelho. Das análises térmicas, efetuadas da temperatura ambiente até 900 °C, verificou-se que o material não apresenta nenhuma mudança de fase e que a decomposição ocorre num processo exotérmico de duas etapas.

Topiramate, a powerful anticonvulsant drug, was investigated by X-ray diffractometry, FT-Raman, FT-IR, TGA and DTA techniques as well as by DFT calculations. From this study it was possible to tentatively assign most of the normal vibrational modes of the crystal. Thermal analysis from room temperature to 900 °C shows that the material does not present any structural phase transition and that the decomposition occurs in a two-step exothermic process.

Keywords: organic crystals, vibrational spectra, X-ray diffraction, thermodynamic properties

Introduction

Epilepsy is a set of neurological disorders that range from brief cessation of responsiveness to severe muscle spasms with a loss of conciousness. In the last years some drugs have been tailored with the objective of controlling epileptic symptoms, the so called anticonvulsant drugs. Among these drugs, one of the most efficient and powerful as antiepileptic is topiramate,[1] a crystalline white powder of molecular formula $C_{12}H_{21}NO_8S$ and structural formula shown in Figure 1. Topiramate (2,3:4,5-bis-*O*-methylethylidene-β-*D*-fructopyranose sulfamate) is derived from a monosaccharide by addition of a sulfamate group, and was discovered by Maryanoff *et al.*[2] in 1987, exhibiting a remarkable anticonvulsant activity. Since the late 1990s it has been used to treat epilepsy (its trade names are
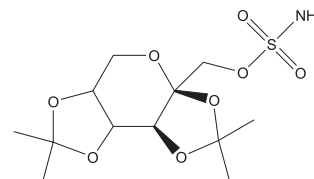

Figure 1. Structural formula of topiramate.

Topamax®, Topimax® or Topamac®) and has recently also been used to prevent migraine headaches in adults.[3]

In the last years, many works have reported physical-chemical characterization of drugs in order to determine several important aspects, such as the influence of processing and formulation of solid pharmaceuticals, polymorphisms, the relationship between physical structures and their properties, among others.[4] Although many clinical properties of topiramate have already been investigated, very few papers address its structural and physical-chemical properties. One of these is from

*e-mail: tarso@fisica.ufc.br

Kubicki *et al.*,[5] which presents a detailed description of its crystal structure obtained from X-ray diffraction data. The crystal belongs to the orthorhombic system, space group $P2_12_12_1$, with cell parameters $a = 7.2497$ Å, $b = 11.0007$ Å, $c = 19.6291$ Å, and $Z = 4$. Also, there are some works published on stability analysis of topiramate,[6] especially on the development of techniques to detect sulfamate and sulfate ions resulting from topiramate decomposition. However, neither thermogravimetric analysis (TGA) nor differential thermal analysis (DTA) results were shown or discussed with regard to possible phase transitions or to further characterize thermal events. On the other hand, Fourier transform (FT)-Raman and FT-infrared (IR) spectroscopies have been used in the last years as alternative techniques to characterize drug molecules, to reveal the solid-state properties arising from polymorphism, and to identify active ingredients and excipients in a drug mixture, among others.[7]

The purpose of this paper is two-fold. First, to present the FT-Raman and FT-IR spectra of topiramate, providing a tentative assignment of the bands observed. Second, we shed light on the thermal behavior of topiramate crystal, in particular, reporting a two-step, exothermic decomposition process.

Experimental

Topiramate (HPLC 99.7%) was provided by Janssen-Cilag Farmacêutica S.A. and used without further purification. In order to obtain the crystals, a saturated aqueous solution was prepared and left to stand at 293 K. Within a week, small, colorless crystals (up to 3 mm on the longest axis), parallelepiped shaped, were collected. X-ray powder diffraction data were collected on a Rigaku D/MAX 2400, using a θ - 2θ geometry, rotating anode source, Cu-K$_\alpha$ radiation (1.542 Å) and scintillation detector. Typical 2θ angular scans ranging from 5 to 75° in varying steps of 0.02° were used in these experiments.

All vibrational measurements were carried out at room temperature. FT-Raman spectra of topiramate were obtained with a Bruker RFS 100/S, using the 1064 nm line of a Nd:YAG laser as exciting source, with a power output of 150 mW. The spectral resolution was set to 4 cm^{-1}, and the signal/noise ratio was enhanced by 60 scans in the range of 70 cm^{-1} to 4000 cm^{-1}. FT-IR spectrum was obtained on a Bruker EQUINOX 55, using a spectral resolution of 4 cm^{-1}. The signal/noise ratio was enhanced by 60 scans from topiramate powder in KBr pellets in the range of 3500 cm^{-1} to 400 cm^{-1}. The vibrational frequencies of the topiramate molecule were calculated by Density Functional

Theory (DFT) using the Gaussian98 package,[8] with the B3LYP method and 6-31G(d,p) basis set, after a suitable geometry optimization. Calculated vibrational spectra (infrared and Raman) were plotted by fitting Lorentzian functions to the peaks, with 10 cm^{-1} FWHM (full width at half maximum). These were graphically (scale factor set to unity) compared to the experimental results and, with the aid of a visualization software, assisted the vibrational assignments.

Crystal samples were analyzed on a SDT Q600, from TA Instruments, performing TGA and DTA simultaneously. The first experimental condition employed was a heating rate of 10 °C min^{-1} under 100 mL min^{-1} nitrogen flux, from 22 to 990 °C. In order to understand the DTA curve around 180 °C in detail, a second condition was employed, with a heating rate of 2 °C min^{-1}, also under 100 mL min^{-1} nitrogen flux, from 19 to 350 °C. In both cases, samples were maintained in a platinum pan.

Results and Discussion

The X-ray powder diffraction pattern obtained from our samples is shown in Figure 2. Sample grinding may have led to some crystals becoming amorphous, which would explain the baseline deviation around 25°. In order to determine whether the sample had the same structure as previously reported in the literature, we calculated all the allowed diffraction angles in the range of 5 to 75° and matched to the observed peaks. Excellent agreement was obtained. The most intense peaks, together with their diffraction planes, are listed in Table 1.

Figure 3 presents the Raman spectrum of the powder sample of topiramate crystal in the range 70-3500 cm^{-1} and
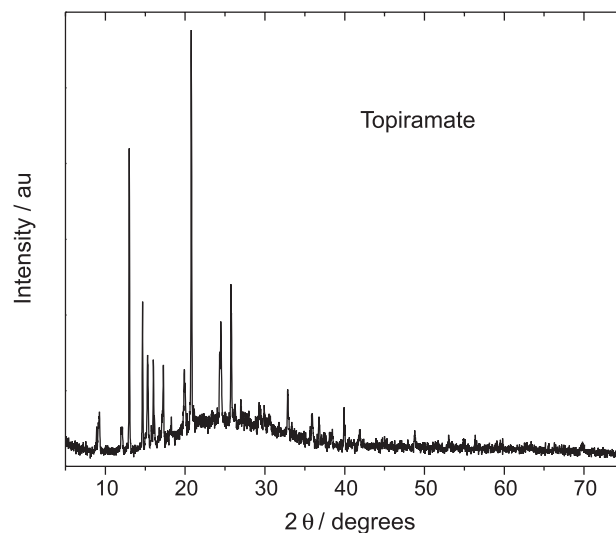

Figure 2. X-ray powder diffraction pattern of topiramate (ground crystals).

Table 1. Predicted diffraction angles for crystalline topiramate, with the corresponding observed angles and planes of reflection

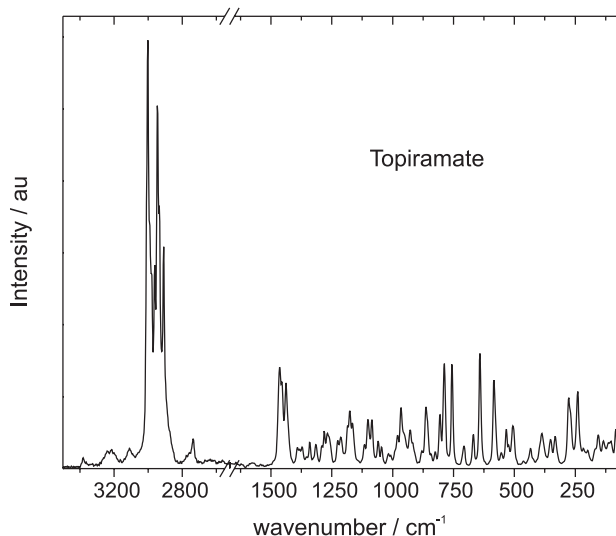| Calc.	Expt.	h k l
9.22	9.26	0 1 1
12.08	12.10	0 1 2
13.02	13.00	1 0 1
14.63	14.66	1 1 0
15.32	15.28	1 1 1
16.11	16.02	0 2 0
17.21	17.28	1 1 2
19.98	19.90	1 1 3
20.77	20.76	1 2 1
24.45	24.48	1 2 3
25.81	25.74	1 0 5
32.88	32.86	0 4 1
35.95	35.94	0 2 7
36.82	36.78	0 3 6
40.03	39.92	0 4 5

Figure 3. FT-Raman spectrum of topiramate powder, showing the range from 70-3500 cm⁻¹, with a break between 1650 and 2550 cm⁻¹.

Figure 4 presents the FT-IR spectrum of topiramate powder in KBr for the spectral region 400-3500 cm⁻¹. Both spectra are shown with an axis break from 1650 to 2550 cm⁻¹ due to absence of peaks and to improve clarity. Modes with wavenumber lower than 150 cm⁻¹ are generally assigned as lattice modes.[9] The tentative assignments of bands observed in the Raman and in the IR spectra of topiramate, based on published vibrational studies on other sulfamates[10-17] and studies on other correlated materials,[18-23] as well as DFT calculations, are given in Table 2. In each case, the most intense band was given a value of 100, and relative intensities are shown in parentheses.
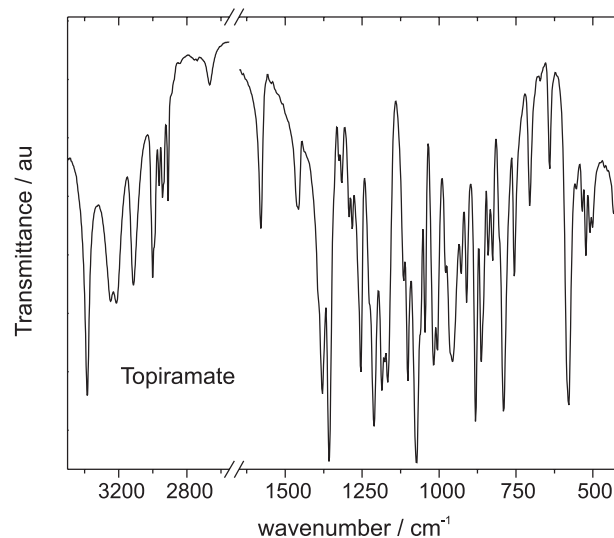
Figure 4. FT-IR spectrum of topiramate powder (KBr pellet) showing the range from 400-3500 cm⁻¹, with a break between 1650 and 2550 cm⁻¹.

According to DFT calculations, the first peaks in this region are associated with C-C torsional motion from methyl groups, at 240, 269, and 278 cm⁻¹, with a considerable contribution of N-S torsion in the first one. However, the N-S torsion is tentatively attributed to the band at 332 cm⁻¹, closer to 300 cm⁻¹ as assigned to other sulfamates,[14,15,17] and accounting for hydrogen bonding effects. The bands at 352 and 386 cm⁻¹ are assigned, respectively, to the SO₃ group symmetric and asymmetric rocking modes, also as in other sulfamates. The angular deformations for this same group are seen at 506 and 554 cm⁻¹ (symmetric), and 585 cm⁻¹ (asymmetric). Angular deformations are also found at 641, 669 and 708 cm⁻¹, involving O-C-O, C-O-C and C-C-O bending. Ring breathing modes are observed, according to DFT, at 756 cm⁻¹ (6-membered-ring) and 788 cm⁻¹ (5-membered-ring).

In the optimized geometry, the N-S bond length (1.668 Å) is close to the one in potassium sulfamate (1.666 Å),[12] but the stretching frequency was calculated at the higher value of 859 cm⁻¹ (unscaled). In the crystal the bond length is 1.576 Å, so this mode was assigned to the band at 806 cm⁻¹. The group of bands 825, 842, 864 and 881 cm⁻¹ are associated with ring deformations due to coupled skeletal stretching and bending modes. Methylene groups rocking modes are assigned separately, the exocyclic one at 928 cm⁻¹ and the endocyclic at a slightly higher frequency of 952 cm⁻¹, due to steric effects from the ring. Rocking from CH₃ groups is observed at 966 and 980 cm⁻¹.

The weak band in the Raman spectrum at 1018 cm⁻¹, with the same frequency but stronger in the infrared, is assigned to stretching of the C-O bond that holds the sulfamate group and agrees very well with the calculated value of 1022 cm⁻¹ (unscaled).

Table 2. Wavenumber (cm⁻¹) and tentative assignment of the bands observed in the FT-Raman and FT-IR spectra of crystalline topiramate at room temperature

Wavenumber/(cm⁻¹) FT-Raman	Wavenumber/(cm⁻¹) FT-IR	Assignment	Wavenumber/(cm⁻¹) FT-Raman	Wavenumber/(cm⁻¹) FT-IR	Assignment
84 (009)	–	lattice modes	1045 (004)	1045 (049)	ν_s SO$_3$
102 (004)	–	lattice modes	1059 (005)	1059 (023)	ν C-O (rings)
114 (004)	–	lattice modes	–	1074 (100)	ν C-O (rings)
134 (005)	–	lattice modes	1085 (010)	–	ν C-O (rings)
155 (007)	–	lattice modes	1097 (003)	–	ν C-O (rings)
169 (002)	–	lattice modes	1102 (009)	1102 (060)	ν C-O (rings)
198 (003)	–	–	1116 (004)	1116 (034)	tw NH$_2$
215 (002)	–	–	1164 (007)	1165 (055)	ν_s SO$_3$
240 (018)	–	τ C-C	1176 (011)	1175 (034)	ν CCC, CCO
269 (010)	–	τ C-C	1186 (006)	1185 (055)	ν_s SO$_3$
278 (014)	–	τ C-C	1213 (005)	1211 (084)	tw CH$_2$, (+ δ CH)
332 (007)	–	τ N-S	1226 (004)	1228 (026)	tw CH$_2$, (+ δ CH)
352 (005)	–	ρ_s SO$_3$	1259 (005)	1254 (057)	ν_{as} SO$_3$
386 (007)	–	ρ_{as} SO$_3$	1268 (006)	1263 (035)	tw CH$_2$, (+ δ CH)
394 (002)	–	–	1281 (007)	1282 (024)	tw CH$_2$, (+ δ CH)
434 (004)	431 (010)	δ CCC	1291 (003)	1293 (022)	tw CH$_2$, (+ δ CH)
463 (001)	–	–	1315 (004)	1316 (017)	δ C-H in phase
–	501 (019)	–	–	1325 (007)	–
506 (010)	510 (018)	δ_s SO$_3$	1340 (005)	–	δ C-H out of phase
523 (002)	523 (030)	–	1354 (001)	1357 (092)	ω CH$_2$
533 (008)	535 (017)	δ C-C-O	1371 (003)	1379 (052)	δ_s CH$_3$ (dimethyl)
554 (002)	554 (012)	δ_s SO$_3$	1382 (003)	–	–
580 (011)	577 (074)	–	1391 (003)	1393 (036)	δ_s CH$_3$ (dimethyl)
585 (017)	586 (050)	δ_{as} SO$_3$	1431 (005)	–	δ_{as} CH$_3$
641 (030)	641 (029)	δ O-C-O (5-ring)	1438 (017)	–	δ_{as} CH$_3$
669 (008)	673 (004)	δ C-O-C (5-ring)	1455 (015)	1458 (029)	δ_s CH$_2$ (exo)
708 (005)	705 (047)	δ C-C-O	1465 (021)	–	δ_s CH$_2$ (endo)
756 (027)	754 (044)	breathing (6-ring)	1581 (001)	1579 (044)	δ_s NH$_2$
788 (026)	790 (089)	breathing (5-ring)	–	2666 (010)	overtone
806 (011)	805 (009)	ν N-S	2739 (006)	2736 (006)	overtone
825 (001)	826 (036)	ring modes	2888 (008)	2844 (001)	overtone
842 (001)	839 (031)	ring modes	2909 (045)	2910 (032)	ν C-H
856 (007)	855 (036)	ring modes	2933 (043)	2934 (017)	ν_s CH$_3$ in phase
864 (013)	863 (054)	ring modes	2945 (075)	2943 (023)	ν_s CH$_3$ in phase
881 (002)	881 (085)	ring modes	2962 (032)	2962 (019)	ν_s CH$_2$ (exo)
910 (001)	910 (044)	–	2979 (028)	–	ν_{as} CH$_2$ (endo)
917 (003)	–	–	2989 (028)	2987 (025)	ν_{as} CH$_3$ out of phase
928 (007)	928 (028)	ρ CH$_2$ (exo)	3003 (100)	3001 (043)	ν_{as} CH$_3$ in phase
952 (006)	951 (056)	ρ CH$_2$ (endo)	3110 (003)	3115 (036)	2 x δ_s NH$_2$
966 (012)	965 (041)	ρ CH$_3$	3210 (003)	3206 (030)	ν_s NH$_2$
980 (005)	979 (023)	ρ CH$_3$	3243 (003)	3251 (039)	ν_s NH$_2$
1008 (001)	1005 (053)	–	3380 (002)	3385 (065)	ν_{as} NH$_2$
1018 (002)	1018 (062)	ν C-O (exo)	–	–	–

ρ = rocking; τ = torsion; ω = wagging; δ = bending; ν = stretching; as = asymmetric; s = symmetric; tw = twisting.

As observed from other sulfamates, the SO$_3$ group gives rise to three symmetric and one asymmetric stretching vibrations. This is due to a lifting of degeneracy by the crystal symmetry. One of each kind was observed in the calculations, the symmetric at 1164 cm^{-1} and the other at 1390 cm^{-1}, coupled to other vibrations. The former was assigned to the band at 1164 cm^{-1}, together with 1045 and 1186 cm^{-1}, and the latter at 1259 cm^{-1}, in better agreement with the literature. The calculated frequency of 1183 cm^{-1} is attributed to CCC and CCO stretching, and tentatively assigned to the peak at 1176 cm^{-1}.

The group of bands from 1059 to 1102 cm^{-1} are associated with C-O stretching from the rings, in agreement with DFT calculations, except for the peak at 1102 cm^{-1} which is shown as a twist from the NH$_2$ group. This mode is assigned to the band at 1116 cm^{-1} in order to account for hydrogen bonding effects, and to be closer to the literature values.

The next group, from 1213 to 1291 cm^{-1}, except for the band at 1259 cm^{-1}, comprises bands assigned to CH$_2$ twisting vibrations, usually coupled to bending of CH, with the modes involving the exocyclic methylene group lying higher in energy than the ones associated to the endocyclic CH$_2$.

Bending vibrations from CH groups are assigned to the bands in 1315 (in phase) and 1340 cm^{-1} (out of phase, Raman only). The very weak peak at 1354 cm^{-1} in the Raman spectrum, but very intense in the infrared, is assigned to the CH$_2$ wagging vibration. Methyl groups symmetric deformations (umbrella) are assigned to the bands at 1371 and 1391 cm^{-1}.

Asymmetric bending from CH$_3$ groups are assigned to bands at 1431 and 1438 cm^{-1}, followed by symmetric bending (scissoring) from methylene groups, the exocyclic at 1455 cm^{-1} and the endocyclic at 1465 cm^{-1}, as in fructopyranose.[22] Last in the low frequency region is the NH$_2$ scissoring mode at 1581 cm^{-1}, one of the highest values as compared to other sulfamates.

The high-wavenumber range (higher than 2700 cm^{-1}) is the region where stretching vibrations of CH$_3$, CH$_2$ and NH$_2$ groups are expected to be observed. As occurs with other materials presenting CH$_2$ and CH$_3$ units, this region is the spectral range where the most intense peaks in the Raman spectra are observed.[9] The stretching vibrations of NH$_2$ are found with the highest energies: the asymmetric stretching is the peak at 3380 and 3385 cm^{-1}, respectively, in the Raman and in the IR spectra. The symmetric stretching, on its turn, is observed as a doublet at 3243 and 3210 cm^{-1} in the Raman spectrum, and at 3251 and 3206 cm^{-1} in the infrared. This is attributed to the fact that, within the crystal, topiramate molecules are held together in linear chains by asymmetric hydrogen bondings (only one of the hydrogens in the amine group participates), running in opposite directions. The peak observed at *ca.* 3110 cm^{-1} can be attributed to an overtone due to Fermi resonance from the amine group scissoring mode, as occurs for other sulphamates.[10,11,14] The asymmetric stretchings of CH$_3$ are observed at 3003 (in phase) and 2989 cm^{-1} (out of phase), followed by the asymmetric stretching of endocyclic CH$_2$ group at 2979 cm^{-1}. The band observed at 2962 cm^{-1} is assigned to the symmetric stretching of exocyclic CH$_2$; this value is almost 30 cm^{-1} higher than that observed for fructopyranose.[20] This is attributed to the presence of the sulfamate group, and supported by the DFT calculations. Additionally, DFT calculations indicate that the peaks at 2933 and 2945 cm^{-1} are associated to symmetric stretching of CH$_3$, while stretching of CH is observed at 2909 cm^{-1}.

The band at 2736 cm^{-1} could be seen as originated from an aldehyde group formed after a partial ring-opening, possibly caused by water in the sample. However, this band is also observed in Raman experiments performed on single crystals (not shown), where the effect of water is negligible, so a possible source for this mode is the overtone of the band at 1371 cm^{-1}. Following the same reasoning, the bands 2666 (infrared only) and 2888 cm^{-1} were also tentatively assigned as overtones.

We also performed a thermal analysis study in order to obtain information about both (*i*) possible polymorphic modification of the material and (*ii*) the decomposition process occurring at high temperatures. It is well known that to screen for polymorphs of a certain crystal we would have to perform crystallization experiments from a diverse range of solvents. Also, for a specific solvent it is possible to obtain crystals with different symmetries depending on parameters such as pH and temperature.[23] However, for each polymorph, the temperatures of the phase transformations are well established and, as a consequence, the thermal analysis is an important tool to search for polymorphism. The discovery of new polymorphs is important because an understanding of the diverse solid state forms can lead to better design and control of drug performance. With these objectives we performed TGA and DTA measurements. In a first run of TGA, a mass loss of 46.8% was observed around 180 °C, followed by a further mass loss of 20.8% in the interval 180-270 °C. Then, mass continues to reduce slowly until the temperature reaches 990 °C, when only 17.8% of the total mass is present. DTA exhibited an endothermic peak at 127.1 °C due to melting of the sample, and another endothermic peak at 177.1 °C, immediately followed by a highly exothermic "loop" at 183.4 °C. This loop is due to a heat release greater than the heating rate of the instrument, which makes it stop heating and then
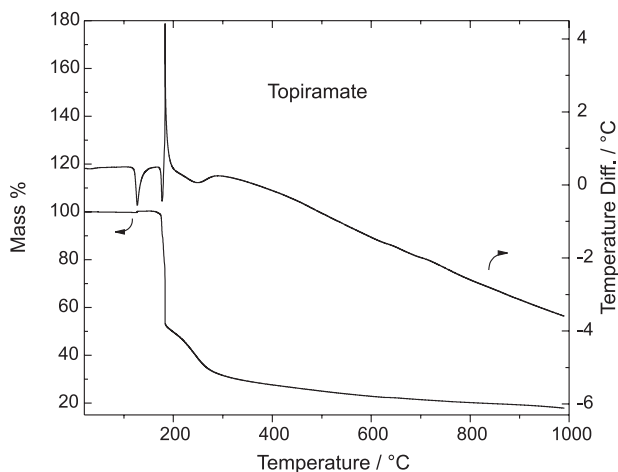
Figure 5. TGA (below, left axis) and DTA (above, right axis) graphs for topiramate, from 22 to 990 °C, at a heating rate of 10 °C min^{-1} and 100 mL min^{-1} nitrogen flux.

recovers after the process is finished. These results are shown in Figure 5.

In order to further shed light on the phenomenon in the region around 180 °C, a lower heating rate was employed. TGA results (not shown) were roughly the same (44.4% mass loss around 180 °C, followed by a 19.7% mass loss up to 260 °C), but DTA recorded melting at 121.4 °C and two sharp exothermic peaks (179.6 and 181.3 °C) instead of the loop just following the endothermic peak at 178.5 °C, as shown in Figure 6.

According to the literature, topiramate melts between 125 and 126 °C.[1] The deviations observed experimentally are due to the different heating rates used, the higher the rate, higher the melting temperature observed. The endothermic peak at 178 °C is attributed to the first stage of decomposition, where topiramate loses the sulfamate group, preceding mass loss. In a second stage,
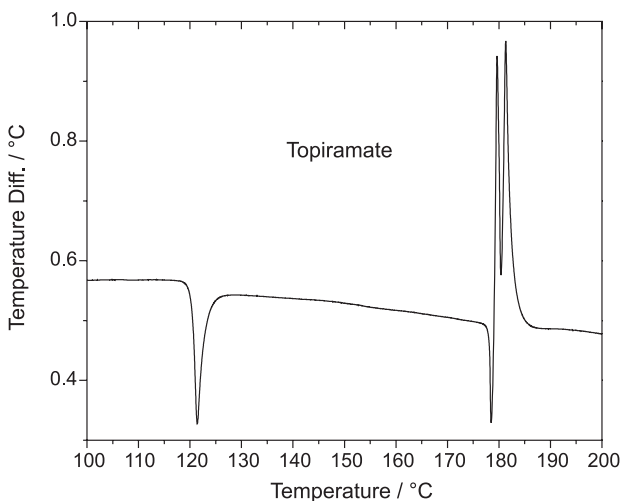
sulfamate decomposes to produce sulfate anions (there is no detectable mass loss here) and the previous molecule (2,3:4,5-bis-*O*-methylethylidene-β-*D*-fructopyranose) decomposes to fructose, thus accounting for the 46.8% mass loss. Thirdly, due to the presence of sulfate ions, we suggest that sulfuric acid is formed and then dehydrates the fructose molecule, accounting for the large volume of the black residue observed at the end of the run. This is proposed in analogy to the dehydration reaction of sugars by sulfuric acid, which is well known to release a large amount of heat and water steam, expanding the charcoal thus formed.

Conclusions

In this letter we have presented vibrational and thermal properties of topiramate, an anticonvulsant drug. From this study, through FT-Raman, FT-IR investigations and DFT calculations, most of observed bands of crystalline topiramate were tentatively assigned. The second main point addressed was the thermal behavior of the material, an important issue for differentiating crystalline modifications, in particular related to materials used as medicines. The sharpness of DTA peaks from the topiramate crystals investigated in this work was a good indication of sample purity. Topiramate thermal stability was verified and no phase transition other than melting was observed. Also, an insight about the decomposition process was provided in this work.

Acknowledgments

References

1. Maryanoff, B. E.; Costanzo, M. J.; Nortey, S. O.; Greco, M. N.; Shank, R. P.; Schupsky, J. J.; Ortegon, M. P.; Vaught, J.L.; *J. Med. Chem*. **1998**, *41*, 1315.

2. Maryanoff, B. E.; Nortey, S. O.; Gardocki, J. F.; Shank, R. P.; Dodgson, S. P.; *J. Med. Chem*. **1987**, *30*, 880.

3. Maryanoff, B. E.; McComsey, D. F.; Costanzo, M. J.; Hochman, C.; Smith-Swintosky, V.; Shank, R. P.; *J. Med. Chem*. **2005**, *48*, 1941.

4. Datta, S.; Grant, D. J. W.; *Nature Rev. Drug Disc*. **2004**, *3*, 42; Dunitz, J. D.; Bernstein, J.; *Acc. Chem. Res*. **1995**, *28*, 193; Brittain, H. G.; *J. Pharm. Sci*. **1997**, *86*, 405.

Figure 6. DTA of topiramate from 19 °C to 350 °C, at a heating rate of 2 °C min^{-1} and 100 mL min^{-1} nitrogen flux.

5. Kubicki, M.; Codding, P. W.; Litster, S. A.; Szkaradzinska, M. B.; Bassyouni, H. A. R.; *J. Mol. Struct.* **1999**, *474*, 255.

6. Micheel, A. P.; Ko, C. Y.; Guh, H. Y.; *J. Chromatogr. B* **1998**, *709*, 166; Klockow-Beck, A.; Nick, A.; Geisshuesler, St.; Schaufelberger, D.; *J. Chromatogr. B* **1998**, *720*, 141; Biró, A.; Pergel, É.; Árvai, G.; Ilisz, I.; Szepesi, G.; Péter, A.; Lukács, F.; *Chromatographia* **2006**, *63*, S137.

7. Pînzaru, S. C.; Pavel, I.; Leopold, N.; Kiefer, W.; *J. Raman Spectrosc.* **2004**, *35*, 338.

8. Frisch, M. J.; Trucks, G. W.; Schlegel, H. B.; Scuseria, G. E.; Robb, M. A.; Cheeseman, J. R.; Zakrewski, V. G.; Montgomery, J. A.; Stratman, R. E.; Vurant, J. C.; Dapprich, S.; Millam, J. M.; Daniels, A. D.; Kudin, K. N.; Strain, M. C.; Farkas, O.; Tomasi, J.; Barone, V.; Cossi, M.; Cammi, R.; Mennuci, B.; Pomelli, C.; Adamo, C.; Clifford, S.; Ochterski, J.; Petersson, G. A.; Ayala, P. Y.; Cui, Q.; Morokuma, K.; Malick, D. K.; Rabuch, A. D.; Raghavachari, K.; Foresman, J. B.; Cioslowski, J.; Ortiz, J. V.; Stefanov, B. B.; Liu, G.; Liashenko, A.; Piskorz, P.; Komaromi, I.; Gomperts, R.; Martin, R. L.; Foz, D. J.; AlLaham, T. M.; Peng, C. Y.; Nanayakkara, A.; Gonzalez, C.; Challacombe, M.; Gill, P. M. W.; Jonson, B.; Chen, W.; Wong, M. W.; Andres, J. L.; Gonzalez, C.; Head-Gordon, M.; Reploge, E. S.; Pople, J. A.; *Gaussian 98, Revision A.11.2*; Gaussian, Inc., Pittsburgh PA, 2001.

9. Lima Jr., J. A.; Freire, P. T. C.; Lima, R. J. C.; Moreno, A. J. D.; Mendes J.; Melo, F. E. A.; *J. Raman Spectrosc.* **2005**, *36*, 1076.

10. Vuagnat, A. M.; Wagner, E. L.; *J. Chem. Phys.* **1957**, *26*, 77.

11. Sundara Raj, A.; Muthusubramanian, P.; Krishnamurthy, N.; *J. Raman Spectrosc.* **1981**, *11*, 127.

12. Sundara Raj, A.; Muthusubramanian, P.; *J. Mol. Struct.* **1982**, *89*, 291.

13. Muthusubramanian, P.; Sundara Raj, A.; *J. Raman Spectrosc.* **1982**, *12*, 24.

14. Muthusubramanian, P.; Sundara Raj, A.; *J. Raman Spectrosc.* **1983**, *14*, 221.

15. Muthusubramanian, P.; Santos, P. S.; Sala, O.; *J. Mol. Struct.* **1984**, *112*, 233.

16. Ilczyszyn, M. M.; Wierzejewska M.; Ciunik, Z.; *Phys. Chem. Chem. Phys.* **2000**, *2*, 3503.

17. Ilczyszyn, M. M.; Ilczyszyn, M.; *J. Raman Spectrosc.* **2003**, *34*, 693.

18. Moreno, A. J. D.; Freire, P. T. C.; Guedes, I.; Melo, F. E. A.; Mendes J.; Sanjurjo, J. A.; *Braz. J. Phys.* **1999**, *29*, 380.

19. Barrett, T. W.; *Spectrochim. Acta* **1981**, *37A*, 233.

20. Baran, J.; Ratajczak, H.; Lutz, E. T. G.; Verhaegh, N.; Luinge, H. J.; van der Maas, J. H.; *J. Mol. Struct.* **1994**, *326*, 109.

21. Söderholm, S.; Roos, Y. H.; Meinander, N.; Hotokka, M.; *J. Raman Spectrosc.* **1999**, *30*, 1009.

22. Benbrahim, N.; Sekkal-Rahal, M.; Vergoten, G.; *Spectrochim. Acta* **2002**, *58A*, 3021.

23. Almeida, F. M.; Freire, P. T. C.; Lima, R. J. C.; Remédios, C. M. R.; Mendes, J.; Melo, F. E. A.; *J. Raman Spectrosc.* **2006**, *37*, 1296.